DE GRUYTER OPEN

Mathematical Modelling in Civil Engineering
Vol. 10-No. 4-2014
Doi: 10.2478/mmce-2014-0020

APPROPRIATE CFD TURBULENCE MODEL FOR IMPROVING INDOOR AIR QUALITY OF VENTILATED SPACES

CĂTĂLIN TEODOSIU – Associate Professor, PhD, Technical University of Civil Engineering, Faculty of Building Services engineering, e-mail: cteodosiu@yahoo.com
VIOREL ILIE – PhD Student, Technical University of Civil Engineering, Faculty of Building Services, e-mail: viorel_ilie_88@yahoo.com
RALUCA TEODOSIU – Lecturer, PhD, Technical University of Civil Engineering, Faculty of Building Services, e-mail:ralucahohota@yahoo.com

Abstract: Accurate assessment of air-flow in ventilated spaces is of major importance for achieving healthy and comfortable indoor environment conditions. The CFD (Computational Fluid Dynamics) technique is nowadays one of the most used approaches in order to improve the indoor air quality in ventilated environments. Nevertheless, CFD has still two main challenges: turbulence modeling and experimental validation. As a result, the objective of this study is to evaluate the performance of different turbulence models potentially appropriate for the prediction of indoor air-flow. Accordingly, results obtained with 6 turbulence models (standard k-ε model, RNG k-ε model, realizable k-ε model, LRN SST k-ω model, transition SST k-ω model and low Reynolds Stress-ω model) are thoroughly validated based on detailed experimental data. The configuration taken into account in this work corresponds to isothermal and anisothermal airflows produced by mixing ventilation systems in small enclosures at low room air changes per hour. In general, the transition SST k-ω model shows the better overall behavior in comparison with measurement values. Consequently, the application of this turbulence model is appropriate for air flows in ventilated spaces, being an interesting option to more sophisticated LES (Large Eddy Simulation) models as it requires less computational resources.

Keywords: turbulence model, CFD, anisothermal jet, ventilation, building

1. Introduction

The basic goal of conditioning enclosed spaces is to supply comfortable and healthy indoor conditions for human beings. This increasingly becomes a vital issue as people spend more time indoors at home, in addition to time spent in shopping malls, theaters, restaurants, vehicles, and other spare time facilities. In fact, recent studies in both Europe and the U.S. clearly show that people spend over 90 percent of their time indoors [1].

On the other hand, it is obvious nowadays that good air quality inside the ventilated spaces cannot be achieved without studies based on modern computational techniques. In line with this, the CFD (Computational Fluid Dynamics) approach is more and more used for analyses concerning: ventilation efficiency for different applications [2-6], indoor air quality for all kind of buildings (e.g. residential [7], offices [8], hospitals [9], museums [10], sport large enclosures [11] or ice skating rinks [12]) and thermal comfort in buildings [13], cars [14], trains [15] or planes [16]. All this is now possible as a result of the remarkable increase in computer hardware capacity in the last years [17].

Despite the fact that the CFD models became useful routinely tools in civil engineering for predicting air movement in ventilated spaces [18], there still are two major challenges. The first one is related to the proper choice of the turbulence model associated to the characteristics of the indoor airflow (e.g. transitional airflow regime, turbulence anisotropy and presence of adverse

pressure gradients) [19]. The second major challenge in CFD is the validation of the numerical results [17].

As a result, the objective of this study is to bring new elements concerning the assessment of different turbulence models for airflows produced by mixing ventilation systems within small enclosures at low room air changes per hour. It is worthwhile to mention that the choice of this configuration is not random. In fact, this allows us to thoroughly study all the critical features mentioned above for the CFD application of turbulent indoor airflows (confined low Reynolds number airflow, with recirculation regions and boundary layer separation). In addition, the judgment of CFD results is based on experimental data validation using a full-scale test room. This responds to the second major challenge concerning the CFD modeling: the lack of verification and validation, particularly in the case of complex airflows.

Consequently, we first present in a succinct manner the experimental set-up, followed by the description of the turbulence models taken into account and their integration in the CFD modeling. We conclude with comprehensive experimental – numerical comparisons in terms of velocity and temperature fields within the ventilated enclosure.

2. Description of the experimental set-up

This work is entirely based on the experimental investigations fulfilled in [20] on indoor air quality in ventilated rooms. It must be said that this study was preferred as it makes available comprehensive experimental data:

- detailed descriptions of the boundary conditions (temperature and flow rate of the supply air, surface temperature on the inside the walls) - required for the numerical model
- velocity and temperature air distributions inside of the room in a vertical plane normal to the center line of the air terminal devices - required for the model validation.

In addition, the tests taken into consideration (see Table 1) correspond perfectly with our objective: study of airflow for mixing ventilation systems within small enclosures at low room air changes per hour. In order to methodically examine the pertinence of the turbulence models taken into account, the tests selected cover all the situations: cold jet, hot jet and isothermal jet (for different low air flow rates) – according to the mean air room temperature.

Table 1

Experimental configurations [20]

Test	$T_0(^0C)$	ACH (h^{-1})	Ar_0	Re_0
B2 (hot jet)	31.4	2.06	0.0032	13566
B4 (cold jet)	9.7	2.02	0.0042	13999
B5 (isothermal jet)	22.3	1.06	0.0005	7106

The physical model is a full-scale test room. The air supply terminal is represented by a commercial diffuser (a grille having an aspect ratio of 12.5), which was placed after a plenum (Fig. 1). Detailed descriptions of the test room and the diffuser are given in [20].

3. CFD model

In view of the fact that this study is focused on the turbulence modeling rather than the CFD model itself, we present only the main characteristics of the numerical approach (see Table 2). All the numerical investigations presented in this work are based on a general-purpose, finite-volume, Navier-Stokes solver (Fluent 15.0.0).

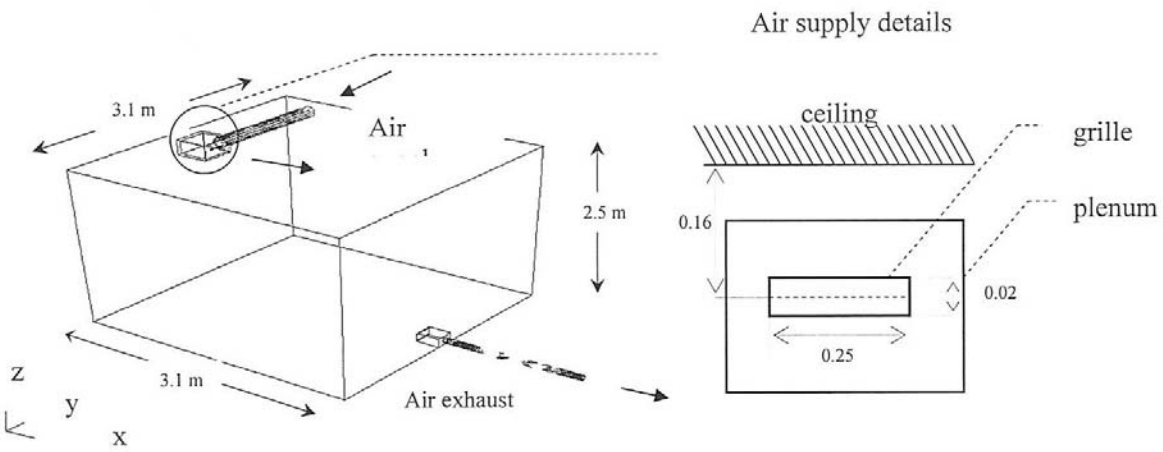

Fig. 1 - Test room and its mixing ventilation system

Table 2

Numerical model principal elements and hypothesis

Feature	Description
Air	Newtonian fluid; incompressible; constant viscosity
Flow	Three-dimensional; steady; non-isothermal; turbulent
Computational domain discretization	Finite volumes; unstructured mesh (tetrahedral elements); optimum mesh size (grid independent solutions); 1300000-1400000 cells
Turbulence model	see section 4: Turbulent air flow modeling
Near wall treatment	k-ε models: two-layer model with enhanced wall functions; k-ω models: no need for special treatment (low Reynolds number corrections)
Numerical resolution	Segregated implicit solver; diffusion terms: second order central-difference scheme; convective terms: second order upwind schemes; velocity-pressure coupling: SIMPLE algorithm; convergence acceleration: algebraic multigrid (gradient method, Green-Gauss cell based)
Air supply boundary conditions	Velocity – fixed value across the diffuser (ratio of the measured air flow rate to the diffuser free area); temperature – uniform value (based on experimental data); turbulence quantities – uniform specification, defining two parameters (turbulence intensity and hydraulic diameter) for all the turbulence models
Air exhaust boundary conditions	Longitudinal exit velocity from mass balance; transverse velocity components are set to zero; gradients normal to flow direction of the other variables are also set to zero
Wall boundary conditions	Velocity – no slip boundary conditions; temperature – fixed values at wall internal surfaces (based on experimental values)

Concerning the construction of the mesh, the size of the smallest cell in the domain is 9.7×10^{-10} m^3 (positioned obviously in the first "chain" of cells within the boundary layer), while the biggest cell is 8.47×10^{-5} m^3. Consequently, the ratio between the smallest and biggest cell in the computational domain is 1.15×10^{-5}.

In addition, we present in Table 3 the values of non-dimensional wall distance (y^+) for the boundary layers of the test room walls. This allows us to estimate the grid suitability for near wall treatment of the flow, in the case of k-ε turbulence models used in conjunction with the approach based on two-layer model. It should be said that the values in Table 3 are representative for all k-ε turbulence models taken into consideration and for all configurations (hot jet, cold jet and isothermal jet).

Table 3

y+ values, B2 test (hot jet), realizable k-ε turbulence model

Wall*	y+ minimum value	y+ maximum value	y+ mean value
east	0.5	18.0	5.2
north	0.6	47.0	10.2
west	0.5	16.7	5.5
south	0.4	18.9	7.9
ceiling	0.3	54.8	9.1
floor	0.5	15.1	6.5

* The surface behind the air supply is considered to be the "south" wall of the test room (the identification of the other walls for the test room is based on this assumption).

4. Turbulent airflow modeling

As stated previously, the airflow within ventilated spaces is extremely complex. This imposes important challenges on turbulence modeling when one wants to use the CFD approach for predicting the convection indoor airflows. In fact, it is hard to have only one turbulence model able to manage all the characteristics of the airflow in ventilated enclosures in an optimal and efficient manner [18]. Consequently, the choice of a turbulence model for the precise calculation of the airflow in ventilated spaces is all the time a compromise between accuracy, hardware resources and computational time. On the other hand, the selection of the right turbulence model depends also on the objective of the analysis. For instance, it is known that for the design and improvement of the airflow in ventilated enclosures the mean air parameters are more useful than the turbulent characteristics of the airflow. Taking all these factors into account, the CFD prediction of the turbulent airflows that occur in enclosed environments can be theoretically performed through three main methods: direct numerical simulation (DNS), large-eddy simulation (LES) and Reynolds-averaged Navier-Stokes (RANS) – divided into two principal types, eddy-viscosity models and Reynolds-stress models [21]. It is worthwhile to note that all these approaches were / are / will be intensely used to predict the air distribution in ventilated enclosures. Nevertheless, the DNS application for complex indoor airflows is impossible now because it demands an extremely fine grid resolution, which leads to unreasonable calculations for the existing computers, in spite of recent advances in the field [22]. The LES approach has been increasingly applied to study airflows in enclosed environments in the last decade. However, the storage and execution time of the LES models are very expensive for real scale 3D indoor flows and their accuracy may not always be the highest [23].

Consequently, in order to accomplish the objective of our study, we performed numerical investigations taking into account several turbulence models based on the RANS approach. These models are detailed below, their integration within the CFD model being performed according to the data from Table 2. For all turbulence models taken into account in this study, the default model constants are used, which are not mentioned here for the sake of brevity.

4.1. RANS Eddy-Viscosity Models

4.1.1. k-ε two-equation model

This turbulence model was the most used and probably the most popular between 1980s and 2000s. The standard k-ε model [24] is based on transport equations for the turbulence kinetic energy (Eq. 1) and its dissipation rate (Eq. 2).

$$\frac{\partial}{\partial t}(\rho k) + \frac{\partial}{\partial x_i}(\rho k u_i) = \frac{\partial}{\partial x_j}\left[\left(\mu + \frac{\mu_t}{\sigma_k}\right)\frac{\partial k}{\partial x_j}\right] + G_k + G_b - \rho\varepsilon - Y_M + S_k \quad (1)$$

$$\frac{\partial}{\partial t}(\rho \varepsilon) + \frac{\partial}{\partial x_i}(\rho \varepsilon u_i) = \frac{\partial}{\partial x_j}\left[\left(\mu + \frac{\mu_t}{\sigma_\varepsilon}\right)\frac{\partial \varepsilon}{\partial x_j}\right] + C_{1\varepsilon}\frac{\varepsilon}{k}(G_k + C_{3\varepsilon} G_b) - C_{2\varepsilon}\rho\frac{\varepsilon^2}{k} + S_\varepsilon \quad (2)$$

The turbulent viscosity is calculated by using the turbulence kinetic energy and its dissipation rate as follows:

$$\mu_t = \rho C_\mu \frac{k^2}{\varepsilon} \tag{3}$$

where C_μ is a constant (0.09).

The standard k-ε model is based on the assumption that the flow is fully turbulent [18], therefore this turbulence model was developed for high Reynolds number flows [22]. As a result, despite its success for numerous engineering applications, the use of standard k-ε model for low Reynolds airflows in enclosed environments leads to unsatisfactory results [25].

4.1.2. RNG k-ε two-equation model

This turbulence model is based on the renormalization group theory [26]. This results in different constants from those in the standard k-ε model. Moreover, there are additional terms and functions in the transport equations for the turbulence kinetic energy (Eq. 4) and its dissipation rate (Eq. 5).

$$\frac{\partial}{\partial t}(\rho k) + \frac{\partial}{\partial x_i}(\rho k u_i) = \frac{\partial}{\partial x_j}\left(a_k \mu_{eff} \frac{\partial k}{\partial x_j}\right) + G_k + G_b - \rho\varepsilon - Y_M + S_k \tag{4}$$

$$\frac{\partial}{\partial t}(\rho \varepsilon) + \frac{\partial}{\partial x_i}(\rho \varepsilon u_i) = \frac{\partial}{\partial x_j}\left(a_\varepsilon \mu_{eff} \frac{\partial \varepsilon}{\partial x_j}\right) + C_{1\varepsilon}\frac{\varepsilon}{k}(G_k + C_{3\varepsilon} G_b) - C_{2\varepsilon}\rho\frac{\varepsilon^2}{k} - R_\varepsilon + S_\varepsilon \tag{5}$$

The turbulent viscosity is computed in this case using a differential equation:

$$d\left(\frac{\rho^2 k}{\sqrt{\varepsilon\mu}}\right) = .72\frac{\hat{v}}{\sqrt{\hat{v}^3 - 1 + C_v}} d\hat{v} \tag{6}$$

where: $\hat{v} = \frac{\mu_{eff}}{\mu}$

Eq. (6) allows the model to improve the prediction of the low Reynolds number and the near-wall flows as the turbulent viscosity varies effectively with the flow eddy scale, depending on the flow characteristics. It is worthwhile to mention that Eq. (6) becomes analogous to Eq. (3), with C_μ = 0.0845 (very close to the value of 0.09 used in the standard k-ε model) for high Reynolds number flows.

The RNG k-ε model has been extensively used for indoor airflows for different configurations [22]. The results agreed generally rather well with the experimental data but there are also several reports about weak performance [19].

4.1.3. Realizable k-ε two-equation model

According to numerous studies [27,28], the implementation of the realizable k-ε model [29] in comparison with the standard k-ε model for flows including boundary layers under strong adverse pressure gradients, separation or recirculation provided superior results. This is supposed to be caused by a new formulation concerning the eddy viscosity and a new model dissipation rate equation, too. In fact, the eddy viscosity is computed using the same equation as in other k-ε models (see Eq. 3) but the major difference is that the coefficient C_μ is no longer constant. Its value is a function of the mean strain and rotation rates, as well as of the turbulence parameters, the turbulence kinetic energy and its dissipation rate. The complete formulation is given in [29]. The modeled transport equation for the dissipation rate of the turbulent kinetic energy is based on the mean square vorticity fluctuation dynamic equation [29]:

$$\frac{\partial}{\partial t}(\rho\varepsilon)+\frac{\partial}{\partial x_j}(\rho\varepsilon u_j)=\frac{\partial}{\partial x_j}\left[\left(\mu+\frac{\mu_t}{\sigma_\varepsilon}\right)\frac{\partial\varepsilon}{\partial x_j}\right]+\rho C_1 S\varepsilon-\rho C_2\frac{\varepsilon^2}{k+\sqrt{v\varepsilon}}+C_{1\varepsilon}\frac{\varepsilon}{k}C_{3\varepsilon}G_b+S_\varepsilon \quad (7)$$

The second term on the right hand side of Eq. (7) does not involve anymore the turbulence kinetic energy production as the other k-ε models. This can lead to more appropriate turbulence length scale descriptions. On the other hand, the transport equation for the turbulence kinetic energy is exactly the same compared to the classical k-ε model (see Eq. 1).

4.1.4. LRN SST k-ω two-equation model

The k-ω models are based on transport equations for the turbulence kinetic energy (Eq. 8) and the turbulence frequency, or specific dissipation rate (Eq. 9).

$$\frac{\partial}{\partial t}(\rho k)+\frac{\partial}{\partial x_i}(\rho k u_i)=\frac{\partial}{\partial x_j}\left(\Gamma_k\frac{\partial k}{\partial x_j}\right)+G_k-Y_k+S_k \quad (8)$$

$$\frac{\partial}{\partial t}(\rho\omega)+\frac{\partial}{\partial x_i}(\rho\omega u_i)=\frac{\partial}{\partial x_j}\left(\Gamma_\omega\frac{\partial\omega}{\partial x_j}\right)+G_\omega-Y_\omega+S_\omega \quad (9)$$

As a result, the turbulent viscosity is computed from these scalars (Eq. 10).

$$\mu_t=\alpha^*\frac{\rho k}{\omega} \quad (10)$$

where the coefficient α* introduces low Reynolds number (LRN) corrections.

The shear-stress transport (SST) k-ω model [30] is based on similar forms for the Eqs. (9) and (10). Nevertheless, this model introduces a damped cross-diffusion derivative term in the specific dissipation rate equation. In addition, there is a modified turbulent viscosity formulation to take into account the transport effects of the turbulent shear stress. These features make the SST k-ω model more appropriate for adverse pressure gradient flows than the standard k-ω model. Consequently, the LRN SST k-ω model has a good potential for predicting indoor environment flows [21].

4.1.5. Transition SST k-ω four-equation model

This recently developed turbulence model is based on the coupling of the SST k-ω model transport equations with two other transport equations [31]: one for the intermittency (Eq. 11) and one for the transition momentum thickness Reynolds number (Eq. 12).

$$\frac{\partial(\rho\gamma)}{\partial t}+\frac{\partial(\rho U_j\gamma)}{\partial x_j}=P_{\gamma1}-E_{\gamma1}+P_{\gamma2}-E_{\gamma2}+\frac{\partial}{\partial x_j}\left[\left(\mu+\frac{\mu_t}{\sigma_\gamma}\right)\frac{\partial\gamma}{\partial x_j}\right] \quad (11)$$

$$\frac{\partial(\rho R\tilde{e}_{\theta t})}{\partial t}+\frac{\partial(\rho U_j R\tilde{e}_{\theta t})}{\partial x_j}=P_{\theta t}+\frac{\partial}{\partial x_j}\left[\sigma_{\theta t}(\mu+\mu_t)\frac{\partial R\tilde{e}_{\theta t}}{\partial x_j}\right] \quad (12)$$

Unfortunately, no study has been found in the literature on the use of this new turbulence model in indoor environments. As a result, this work makes available extremely valuable data on the application of the transition SST k-ω model for ventilated spaces.

4.2. RANS Reynolds-stress models

The Reynolds-stress models (RSM) are generally based on 7 equations: six transport equations for the Reynolds stresses and one transport equation for a turbulent quantity (the dissipation rate of turbulence energy or the turbulence frequency). Consequently, the RSM models allow the "natural" development and transport of individual Reynolds stresses, which allow taking into account the anisotropy of turbulent flows. These anisotropic effects play an important role in

flows with significant buoyancy, streamline curvature, swirl or strong circulation [21]. The correct prediction of these effects leads normally to more accurate results for complex indoor airflows compared with two-equation turbulence models [18].

4.2.1. Low Reynolds Stress-ω model

The RSM model selected in this study to solve transport equations for the individual Reynolds stresses is the low-Reynolds Stress-ω by Wilcox [32]. This model is based on the transport equation for the specific dissipation rate (Eq. 9) and the Launder-Reece-Rodi (LRR) stress-transport model. The model closure coefficients are identical to the k-ω model. However, the low-Reynolds Stress-ω model requires additional closure coefficients. The comprehensive physical-mathematical formulation of the model can be found in [32]. It is worthwhile to mention that this model was used with good results for the prediction of room air movement induced by a wall jet [19].

5. Results

The comparisons between numerical results and experimental values are exposed in terms of air mean velocity and temperature profiles in a median vertical plane for three sections located at different distances from the coordinate system presented in the Fig. 1. The exact position of these rakes is shown in Fig. 2.

It is worthwhile to mention that we focus our validation on air mean velocity and air temperature as these parameters represent the main issues to assess the efficiency of ventilation systems - deeply related to indoor air quality and thermal comfort in ventilated spaces.

We first present in Fig. 3 the data for the isothermal situation (velocity profiles). We notice that the jet region (including its spread) is correctly predicted by the k-ε realizable model in the first section (at x = 1 m) while there are 3 turbulence models (k-ε realizable model, transition SST k-ω and low Reynolds stress-ω model) with good performance at x = 1.8 m and x = 2.7 m.

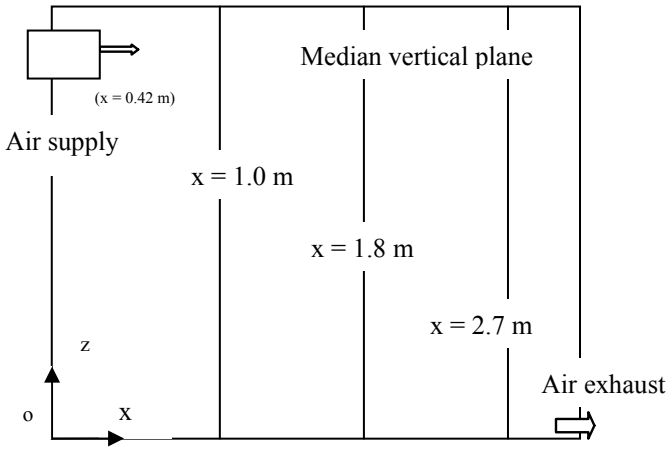

Fig. 2 – Results sections

Concerning the comparisons between predicted and measured values for the hot jet, the velocity profiles and temperatures profiles are shown in Figs. 4 and 5, respectively. In the closest section from the air supply (x = 1 m), the low Reynolds stress-ω model has slightly the best velocity predictions. Nevertheless, as a general remark, the k-ω models (low Reynolds number shear-stress transport – LRN SST and transition SST) show the best agreement with measurements both for velocity and temperature.

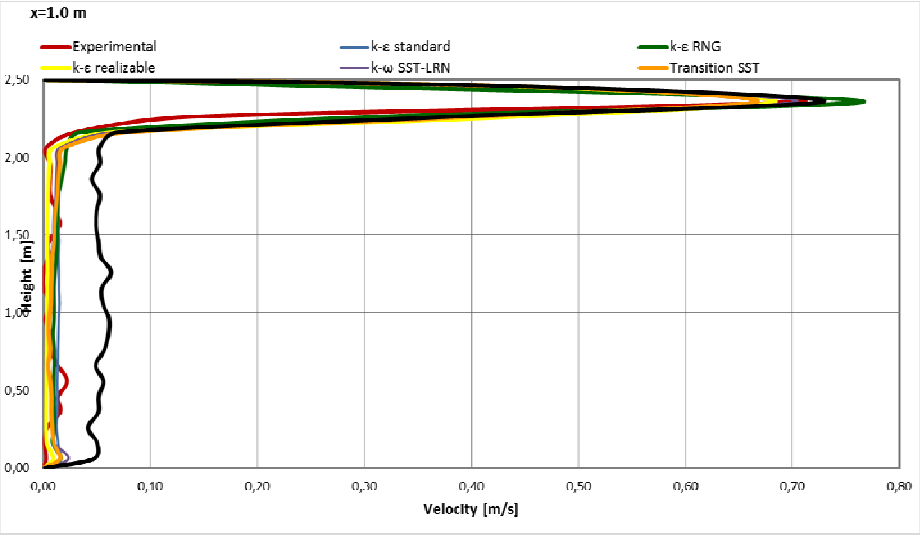

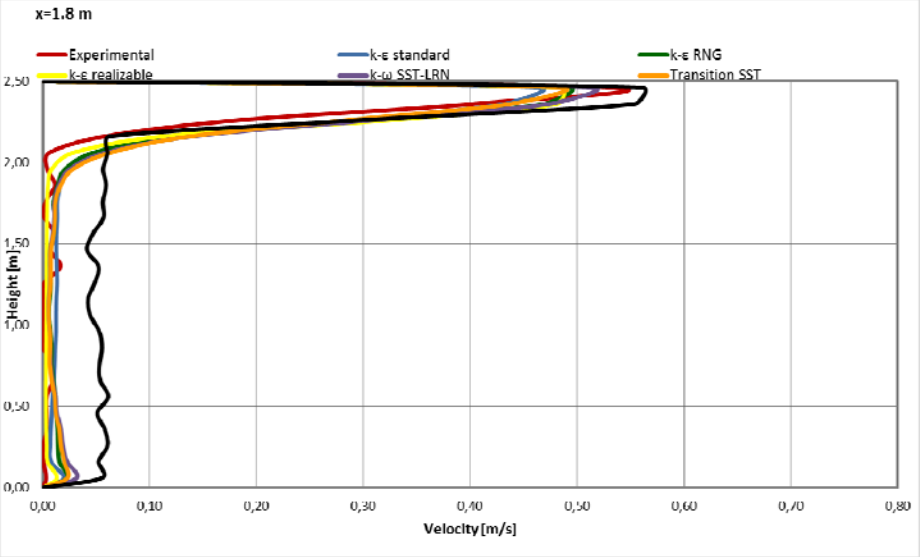

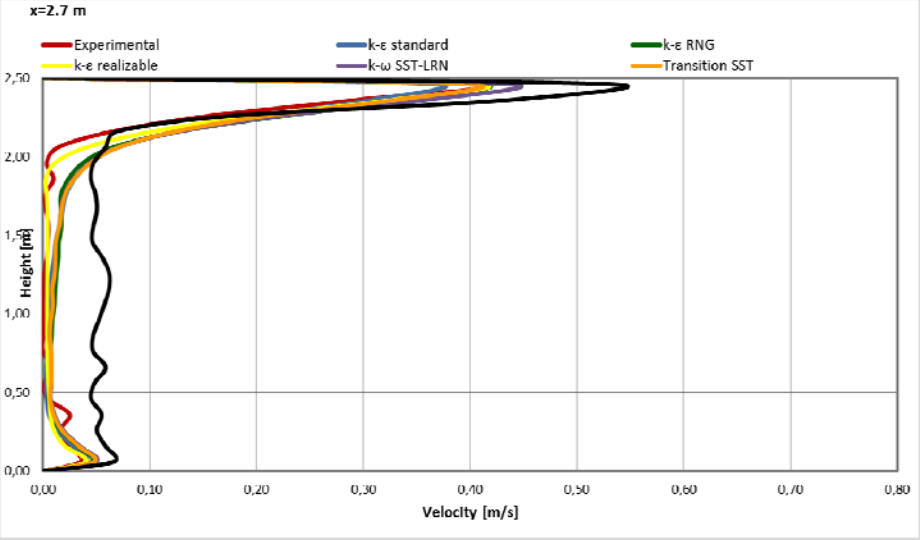

Fig. 3 –Velocity profiles (B5 - isothermal jet test)

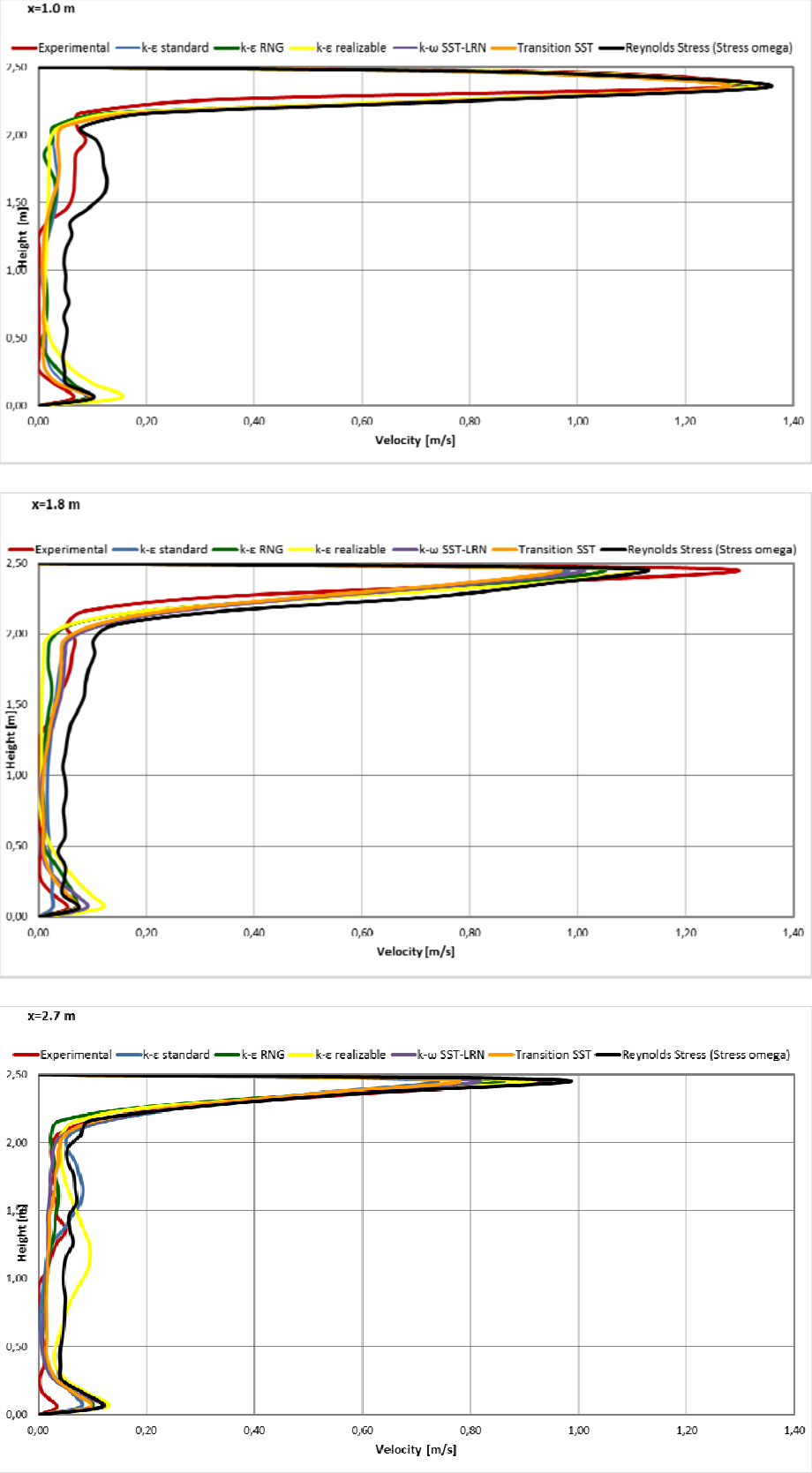

Fig. 4 – Velocity profiles (B2 – hot jet test)

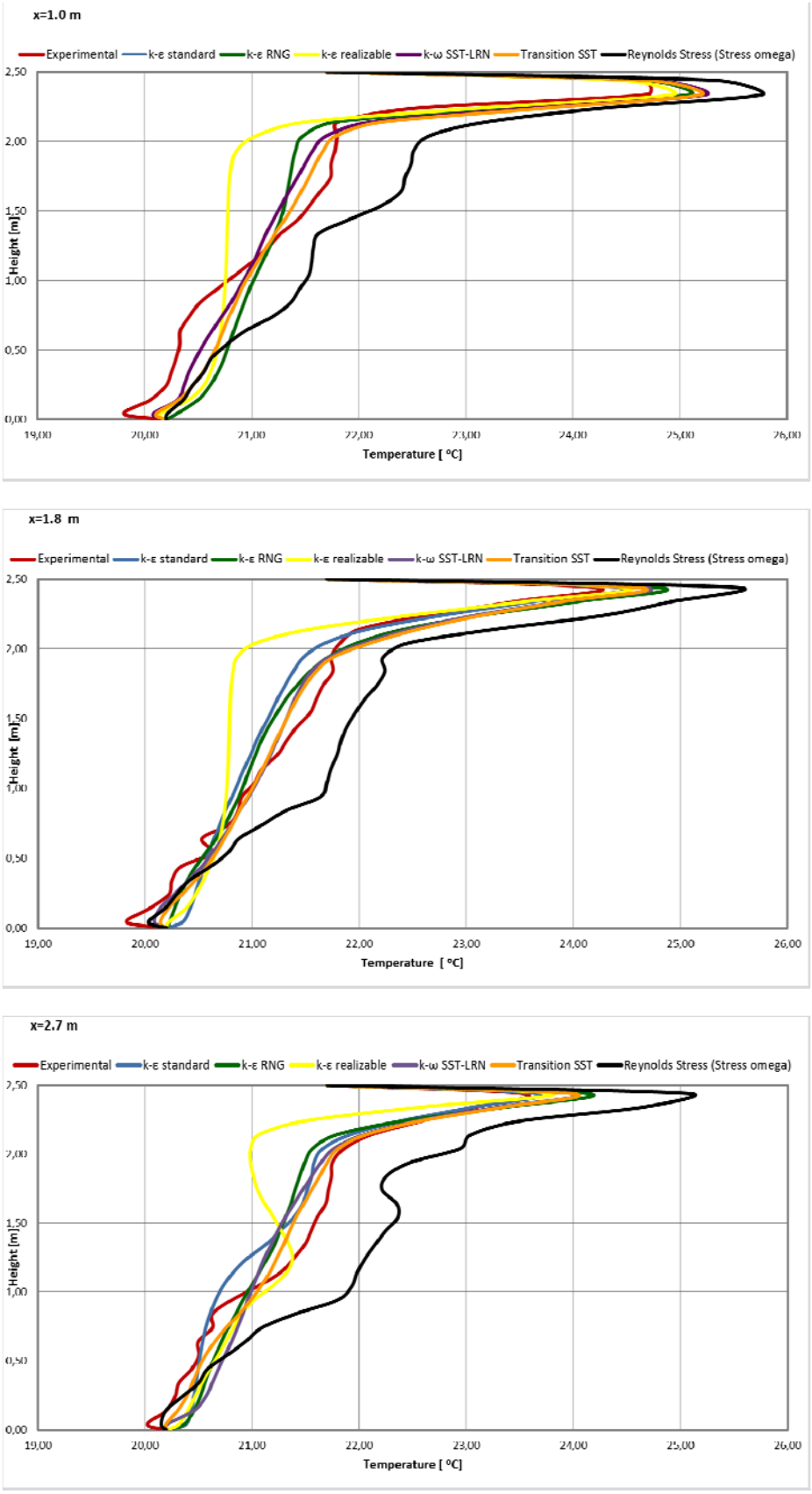

Fig. 5 – Temperature profiles (B2 – hot jet test)

For the more complex airflow, which occurs in the case of a cold jet supplied in the room (Figs. 6 and 7), there is now a turbulence model capable to predict the overall flow pattern in the enclosure. However, there are 3 models that lead to results in better agreement with experimental

data: transition SST k-ω, low Reynolds stress-ω and k-ε realizable (the last one only in the section at x = 2.7 m).

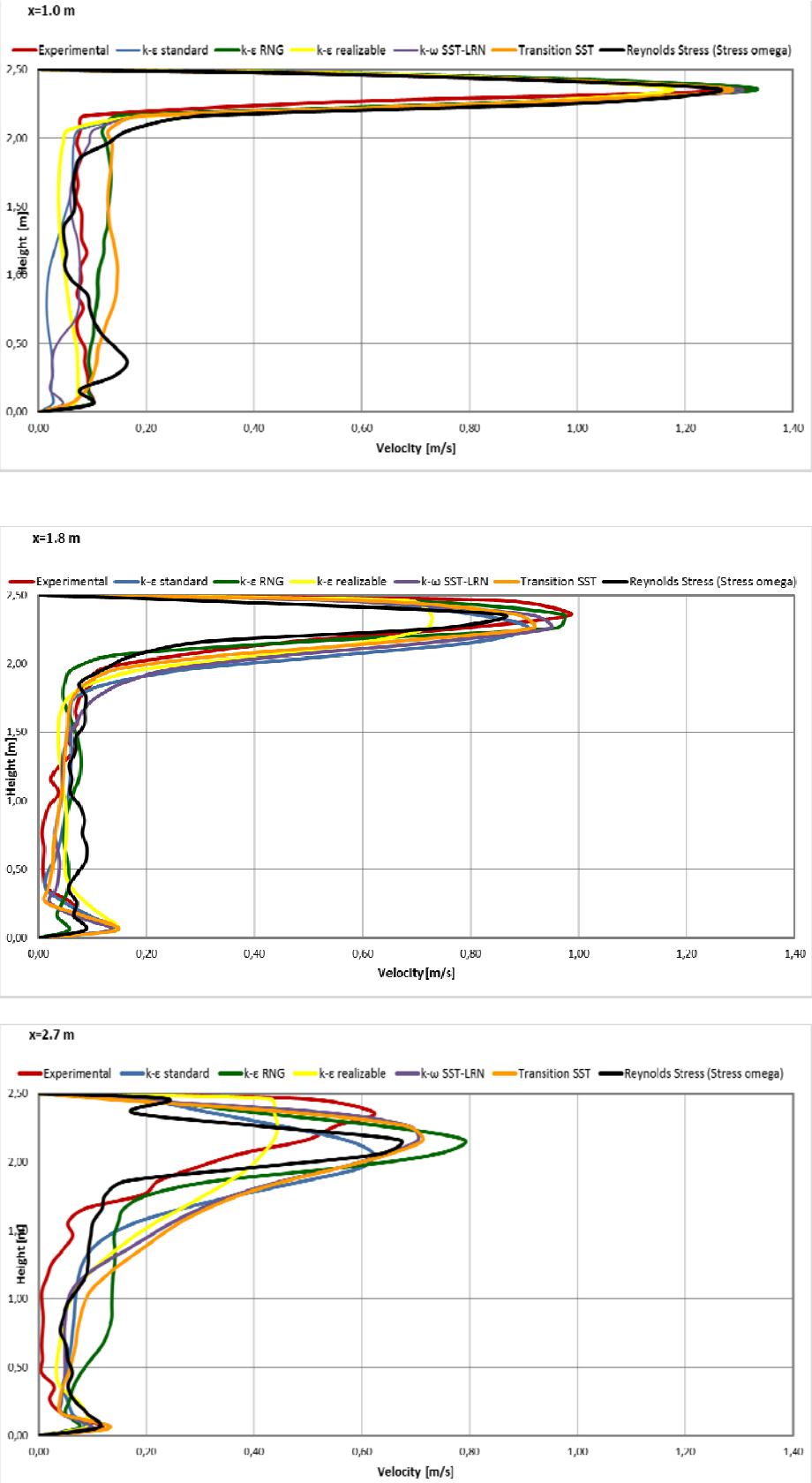

Fig. 6 – Velocity profiles (B4 – cold jet test)

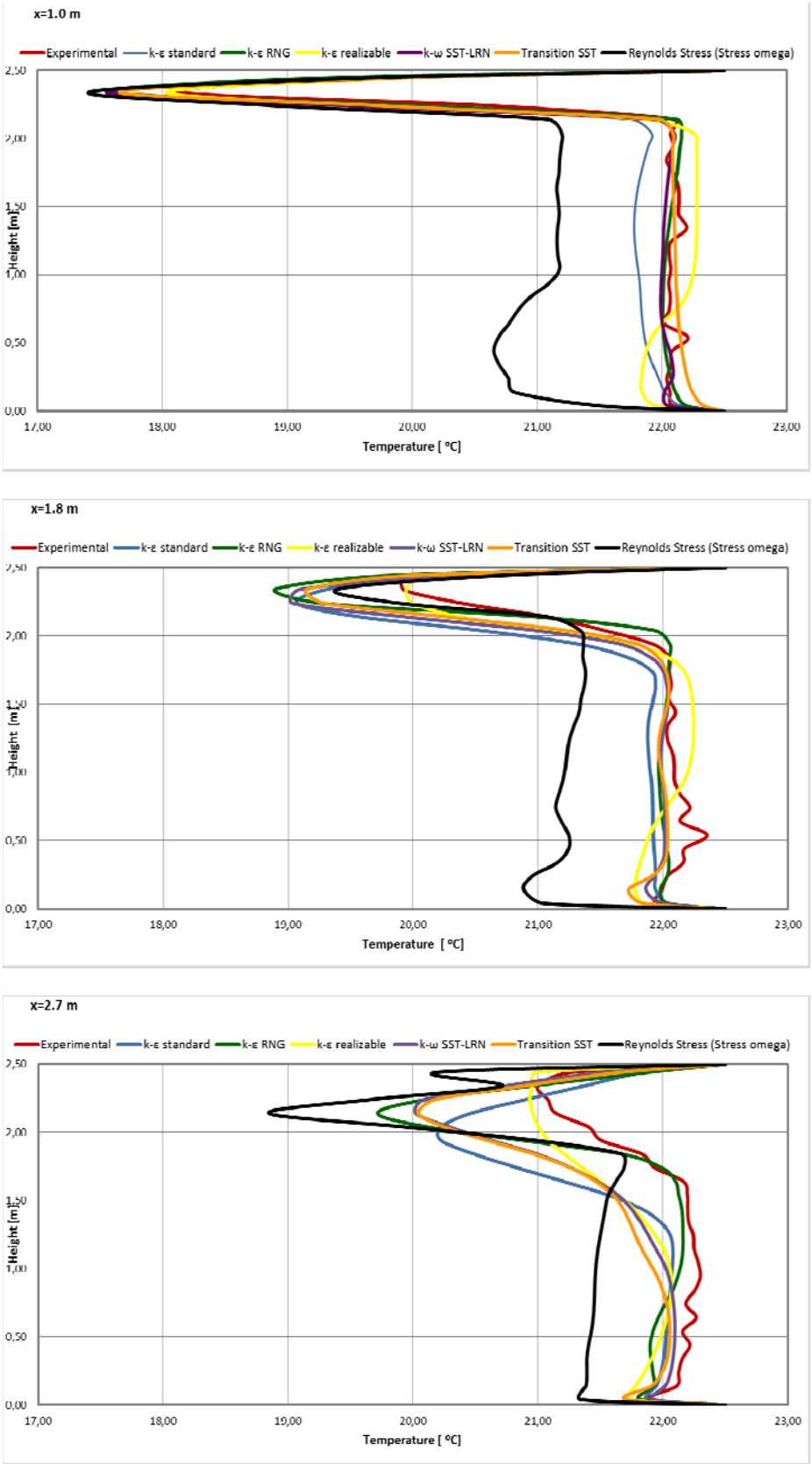

Fig. 7 – Temperature profiles (B4 – cold jet test)

6. Conclusions

Despite the expectations, none of the turbulence models taken into consideration provide entirely superior results for the mean velocity and temperature fields in the ventilated test room. We include here as well the Reynolds-stress model although the results obtained with this model show in general fair agreement with experimental data. Nevertheless, the prediction of the airflow for all the 3 configurations taken into account based on the Reynolds-stress turbulence model deviates sometimes a lot from the measurements. The same comment is found in [19].

On the other hand, from the results it is noted that the k-ω models (especially the transition SST model) have the best average overall performance in comparison with the measurements, no matter the configuration (isothermal jet, hot jet or cold jet). This indicates that the k-ω models present a good potential to model indoor airflow in ventilated spaces even if the studied configuration is highly complex due to the presence of transitional flow, adverse pressure gradient, and a wall jet that is basically anisotropic. The results of this study show that the transition SST k-ω model clearly improves the predictions concerning the temperature distributions, based usually on k-ε models. This theory is confirmed also by [21, 33].

In conclusion, the new transition SST k-ω four-equation model should be methodically applied for indoor environments with complex airflows in future work in order to better validate its performance. This turbulence model can represent an interesting alternative to LES turbulence models for indoor airflow as it demands less computational resources.

Nomenclature

ACH	air changes per hour, h^{-1}
Ar_0	Archimedes number (based on inlet dimensions)
C_1, C_2, $C_{1\varepsilon}$, $C_{2\varepsilon}$, $C_{3\varepsilon}$, C_ν, C_μ	k-ε models coefficients
$E_{\gamma 1}$, $E_{\gamma 2}$	transition SST k-ω source terms
G_b, G_k, G_ω	k-ε and k-ω source terms
k	turbulent kinetic energy, m^2/s^2
$P_{\gamma 1}$, $P_{\gamma 2}$, $P_{\theta t}$	transition SST k-ω source terms
Re_0	Reynolds number (based on inlet dimensions)
$Re_{\theta t}$	transition momentum thickness Reynolds number
R_ε	RNG k-ε model source term for RNG theory
S, S_k, S_ε, S_ω	k-ε and k-ω models user source terms
t	time, s
T_0	inlet air temperature (°C)
$u_{i,j}$	air velocity components, m/s
$x_{i,j}$	coordinates
Y_K, Y_M, Y_ω	k-ε and k-ω models source terms

Greek symbols

α^*	LRN SST k-ω model LRN corrections coefficient
α_K, α_ε	RNG k-ε model – inverse effective Prandtl numbers for k and ε
ε	dissipation of turbulent kinetic energy, m^2/s^3
Γ_K, Γ_ω	LRN SST k-ω model – effective diffusivity for k and ω
γ	intermittency
μ	laminar (molecular) viscosity
μ_{eff}	effective viscosity
μ_t	turbulent (eddy) viscosity
ν	cinematic viscosity
ρ	density, kg/m^3
σ_K, σ_ε, σ_γ, $\sigma_{\theta t}$	k-ε model and transition SST k-ω model coefficients
ω	turbulence frequency (specific turbulence dissipation rate), s^{-1}

Acknowledgments

This work was supported by a grant of the Romanian Ministry of Education and Research, CNCS-UEFISCDI, project number PN-II-ID-JRP-RO-FR-2012-0071.

References

[1] Hancock, T. (2002). *Built Environment (Encyclopedia of Public Health).* Retrieved June 19, 2014 from http://www.encyclopedia.com/doc/1G2-3404000130.html

[2] Rota R., Canossa L. & Nano G. (2001). Ventilation design of industrial premises through CFD modelling. *Canadian Journal of Chemical Engineering*. 79(1), 80-86.

[3] Kaji H., Akabayashi S.I. & Sakaguchi J. (2009). CFD analysis for detached house: Study on the ventilation efficiency on constantly ventilated house part 1. *Journal of Environmental Engineering*. 74(636), 161-168

[4] Papanikolaou E., Venetsanos A.G., Cerchiara G.M., Carcassi M. & Markatos N. (2011). CFD simulations on small hydrogen releases inside a ventilated facility and assessment of ventilation efficiency. *International Journal of Hydrogen Energy*. 36(3), 2597-2605

[5] Kwon K.S., Lee I.B., Han H.T., Shin C.Y., Hwang H.S., Hong S.W., Bitog J.P., Seo I.H. & Han C.P. (2011). Analysing ventilation efficiency in a test chamber using age-of-air concept and CFD technology. *Biosystems Engineering*. 110(4), 421-433.

[6] Zhai Z.Q. & Metzger I.D. (2012). Taguchi-Method-Based CFD Study and Optimisation of Personalised Ventilation Systems. *Indoor and Built Environment*. 21(5), 690-702.

[7] Yang L., Ye M. & He B.J. (2014). CFD simulation research on residential indoor air quality. *Science of the Total Environment*.472, 1137-1144.

[8] Zhuang R., Li X. & Tu J. (2014). CFD study of the effects of furniture layout on indoor air quality under typical office ventilation schemes. *Building Simulation*. 7(3), 263-275.

[9] Helmis C.G., Adam E, Tzoutzas J, Flocas H.A., Halios C.H, Stathopoulou O.I., Assimakopoulos V.D., Panis V., Apostolatou M. & Sgouros G. (2007). Indoor air quality in a dentistry clinic. *Science of the Total Environment*. 377(2), 349-365.

[10] Corgnati S.P. & Perino M. (2013). CFD application to optimise the ventilation strategy of Senate Room at Palazzo Madama in Turin (Italy). *Journal of Cultural Heritage*. 14(1), 62-69.

[11] Stathopoulou O. I. & Assimakopoulos V. D. (2008). Numerical Study of the Indoor Environmental Conditions of a Large Athletic Hall Using the CFD Code PHOENICS. *Environmental Modeling & Assessment*. 13(3), 449-458.

[1] Yang C., Demokritou P.,Chen Q., Spengler J. & Parsons A. (2000). Ventilation and air quality in indoor ice skating arenas. ASHRAE Transactions, 106, p. 338

[2] Cheng Y., Niu, J. & Gao N. (2012). Thermal comfort models: A review and numerical investigation. Building and Environment. 47(1), 13-22.

[3] Lombardi G., Maganzi M., Cannizzo F. & Solinas G. (2009). CFD simulation for the improvement of thermal comfort in cars. Auto Technology. 9(2), 52-56.

[4] Chen N., Liao S. & Rao Z. (2012). CFD evaluation on the temperature field and thermal comfort of coach in low atmospheric pressure passenger trains with oxygenation at high altitudes. China Railway Science. 33(4), 126-132.

[5] Sun H., An L., Feng Z. & Long Z. (2014).CFD simulation and thermal comfort analysis in an airliner cockpit. Journal of Tianjin University Science and Technology. 47(4), 298-303.

[6] Li Y. & Nielsen P.V. (2011).CFD and ventilation research. Indoor Air. 21, 442-453.

[12] Sørensen D.N. & Nielsen P.V. (2003). Quality control of computational fluid dynamics in indoor environments. *Indoor Air*. 13, 2-17.

[13] van Hooff T. Blocken B. & van Heijst G.J.F. (2013). On the suitability of steady RANS CFD for forced mixing ventilation at transitional slot Reynolds numbers. *Indoor Air*. 23, 236-249.

[14] Castanet S. (1998). *Contribution to the study of ventilation and indoor air quality*. Doctoral dissertation, INSA de Lyon, Villeurbanne, France.

[15] Stamou A. & Katsiris I. (2006). Verification of a CFD model for indoor airflow and heat transfer. *Building and Environment*. 41, 1171-1181.

[16] Zhai Z., Zhang Z., Zhang W. & Chen Q.Y. (2007). Evaluation of Various Turbulence Models in Predicting Airflow and Turbulence in Enclosed Environments by CFD: Part 1 – Summary of Prevalent Turbulence Models. *HVAC&R Research*. 13(6), 853-870.

[17] Zhang Z, Zhang W., Zhigiang J.W. & Chen Q.Y. (2007).Evaluation of Various Turbulence Models in Predicting Airflow and Turbulence in Enclosed Environments by CFD: Part 2—Comparison with Experimental Data from Literature. *HVAC&R Research*. 13(6), 871-886.

[18] Launder B.E. & Spalding D.B. (1972). *Lectures in Mathematical Models of Turbulence*. London, England: Academic Press

[19] Schälin A. & Nielsen P.V. (2004). Impact of turbulence anisotropy near walls in room air flow. *Indoor Air*. 14(3), 159-168.

[20] Yakhot V. & Orszag S.A. (1986). Renormalisation group analysis of turbulence. *Journal of Science Computing*. 1(1), 3-51.
[21] Teodosiu C., Rusaouen G. & Hohotă R. (2003). Influence of boundary conditions uncertainties on the simulation of ventilated enclosures. *Numerical Heat Transfer, Part A: Applications – An International Journal of Computation and Methodology*. 44, 483-504.
[22] Hussain S. & Oosthuizen P.H. (2012). Validation of numerical modeling of conditions in an atrium space with a hybrid ventilation system. *Building and Environment*. 52, 152-161.
[23] Shih T.H., Liou A., Shabbir A., Yang Z. & Zhu J. (1995). A new k-ε Eddy-Viscosity Model for High Reynolds Number Turbulent Flows - Model Development and Validation. *Computers Fluids*. 24(3), 227-238.
[24] Menter F.R. (1994). Two-Equation Eddy-Viscosity Turbulence Models for Engineering Applications. *AIAA Journal*. 32(8), 1598-1605.
[25] Langtry R.B. & Menter F.R. (2009). Correlation-Based Transition Modeling for Unstructured Parallelized Computational Fluid Dynamics Codes. *AIAA Journal*. 47(12), 2894-2906.
[26] Wilcox D.C. (1998). *Turbulence Modeling for CFD*. La Canada, California, USA: DCW Industries, Inc.
[27] Hussain S., Oosthuizen P.H. & Kalendar A. (2012). Evaluation of various turbulence models for the prediction of the airflow and temperature distributions in atria. *Energy and Buildings*. 48, 18-28.